May 2016

The Influence of Currents and Bathymetry on the Phytoplankton Growth Dynamics in a Deep Lake: An Application of the Lattice Boltzmann Method

Breanna Patrice Swan
University of Wisconsin-Milwaukee

THE INFLUENCE OF CURRENTS AND BATHYMETRY ON THE PHYTOPLANKTON GROWTH DYNAMICS IN A DEEP LAKE: AN APPLICATION OF THE LATTICE BOLTZMANN METHOD

by

Breanna Swan

A Thesis Submitted in

Partial Fulfillment of the

Requirements for the Degree of

Master of Science

in Mathematics

at

The University of Wisconsin-Milwaukee

May 2016

ABSTRACT

THE INFLUENCE OF CURRENTS AND BATHYMETRY ON THE PHYTOPLANKTON GROWTH DYNAMICS IN A DEEP LAKE: AN APPLICATION OF THE LATTICE BOLTZMANN METHOD

by

Breanna Swan

The University of Wisconsin-Milwaukee, 2016
Under the Supervision of Professor Lauko

The invasive species, the quagga mussel, infiltrated Lake Michigan in the early 2000s and immediately began depleting the base of the aquatic food system: the lake's phytoplankton population. Today the quagga mussel covers 80% of the lake floor deeper than 10 meters, can be concentrated at 35,000 mussels per square meter, and is efficient at filtering throughout the depth of the water column. This thesis aims to contribute to the difficult task of describing the impact these mussels have on the size and preferred depth of the phytoplankton population in Lake Michigan. In a simplified model, two species of phytoplankton competing for nutrients (one preferred) with bottom boundary mussel consumption were simulated using the lattice Boltzmann method. Four lake-bottom boundary condition scenarios, the Mid Lake Plateau, an open channel, a small hill, and a steep drop-off, were considered in order to test the viability and flexibility of the lattice Boltzmann method and to explore how the bathymetry of Lake Michigan influences the phytoplankton population. In addition, slow and fast currents were tested and the varying distributions of the phytoplankton were analyzed. The results of this thesis can be used to evaluate the viability of a modeling and computational tool for quantitatively evaluating the impacts bathymetry and currents have on an aquatic system.

DEDICATION

To my fiance who is my voice of reason and source of reassurance, to my family who used their mathematical and grammatical expertise to support my love of math and research, and to Charlotte and Bryce who remind me life is better with a smile.

TABLE OF CONTENTS

LIST OF FIGURES

LIST OF TABLES

LIST OF ABBREVIATIONS

LBM ..... lattice Boltzmann method

P1 ..... Phytoplankton species 1

P2 ..... Phytoplankton species 2

N1 ..... Nutrient 1, Ammonia

N2 ..... Nutrient 2, Nitrate

ACKNOWLEDGEMENTS

First and foremost I would like to thank my advisor, Dr. Lauko, for meeting with me consistently throughout the year-long research project, providing knowledge and resources for the background of this project, and working with me to overcome MATLAB barriers.

Thank you to Dr. Gabriella Pinter and Tom Stojsavljevic who continue to be a part of the larger Lake Michigan phytoplankton project in the mathematics department and who provided to me the biological model and parameters for this thesis.

Thank you to my friends and colleagues, Martin and Bryan, for listening to my coding woes during the creation process and providing ideas or support in order to break through the roadblocks and find success.

1 Introduction

1.1 Relevance

Ingesting and recycling nutrients, modifying the shape and habitat of the bottom layer of water, and disrupting the original food system are a few of the ways dressenid mussels have negatively altered the Great Lakes since its invasion in the early 2000s [25, 26, 33, 37]. Zebra mussels were the first dressenid mussels to invade Lake Michigan but recently were out-competed by their more resilient counterparts, the quagga mussel (*Dreissena rostriformis bugensis*), which flourishes in both shallow and deep cool water [31].

Quagga mussels are bottom living filter feeders who consume the base nutrient of most aquatic food systems: the phytoplankton population. The quagga mussel is efficient at filtering nutrients from the entire water column and will consume 100 % of the organic matter that falls to the lake floor [31, 35, 36]. A recent screening of the bottom of Lake Michigan showed that quagga mussels cover 80 % of the lake floor deeper than 10 meters [25].

One example of the negative effects this invasion of mussels has had on Lake Michigan is the disappearance of the spring phytoplankton bloom. This change in the aquatic system has resulted in low population counts for the larger invertebrate species of Lake Michigan who usually thrive off of the yearly bloom [29]. One could argue that a positive aspect of the quagga mussel invasion is an increase in water transparency and cleanliness due to the high volume of water being filtered by the mussels [3, 11]. Even so, the negative environmental effects greatly outweigh the positives. It is critical that an accurate model of the interactions between dressenid mussels, phytoplankton, and freshwater nutrients be created in order to develop strategies to protect all species who depend on the phytoplankton population to survive.

The lattice Boltzmann Method is a successful way to model fluid dynamics. The main concept of this project was to use a straightforward and computationally efficient lattice

Boltzmann model to compute fluid fluxes generated over various boundary features from the lake current and, from these fluxes, obtain fluxes for the dissolved and suspended nutrient and phytoplankton densities within the water. Additionally, the model will incorporate the major bio-reactions impacting the base of the food system such as the light and nutrient-controlled phytoplankton growth and the influence of mussel grazing and nutrient recycling impacting the system from the boundary of the fluid domain.

1.2 The lattice Boltzmann Method

In the last 20 years, the lattice Boltzmann method has become a popularized way of solving transport equations, including fluid flow, due to its connection between the macroscopic Navier-Stokes type systems of equations and the microscopic properties and interactions governed by Hamilton's equations [1,21,40]. The difficulty in solving Navier-Stokes systems of partial differential equations is the non-linearity in convection-diffusion terms and complex geometries imposed by boundary conditions. In contrast, it would be computationally expensive and time-consuming to keep track of each spatial position and velocity vector for each particle at the microscopic scale. The primary function of the lattice Boltzmann method is to model the kinetic energies of microscopic processes such that the macroscopic qualities of conservation of mass, momentum, and energy are obeyed through describing the particles within the macroscopic system as a distribution function [21].

Numerical results have shown that the lattice Boltzmann method discretized in time and space is just as accurate and the computational time similar to the finite-difference approximation of the Navier-Stokes equations [13]. The LBM is a computationally straightforward, flexible, and a highly parallelizable method for solving Navier-Stokes fluid flow problems.

lattice gas automata

The lattice Boltzmann method was developed from lattice gas automata which is a kinetic system in discretized space and time. The space is divided into a lattice while the set of boolean (True/False) variables describe the occupancy of a particle at each lattice node throughout the space. Particles can only move from one lattice node to another and there can only be 1 or 0 particles at each node in each time step.

$$n_\alpha(\mathbf{x}, t) = 0 \qquad \text{no particle at node x and time t} \tag{1}$$

$$n_\alpha(\mathbf{x}, t) = 1 \qquad \text{node is occupied by a particle at time t} \tag{2}$$

for $\alpha = [0, ..., M]$ where M is the number of possible directions a particle can travel from any node. The space and time evolution for the particles in the lattice can be described as:

$$n_\alpha(\mathbf{x} + \mathbf{e}_\alpha \delta t, t + 1) = n_\alpha(\mathbf{x}, t) + \Omega_\alpha n_\alpha(\mathbf{x}, t) \tag{3}$$

with e_α local particle velocity directions, δt time step, and Ω_α the collision operator [21].

In lattice gas automata, the collision term can only have three values, -1 if a particle leaves, 0 if nothing changes, and 1 if a particle is added to that node. All interactions are local, thus, there are no interactions between next-nearest neighbors and collisions are independent of the magnitude of velocity. In other words, the particles' velocity is the same as the grid speed and, as such, will only move one node away for each time step. The evolution of the lattice gas particles occurs as two steps: collision and stream. During streaming, particles move to the closest node in the direction of its velocity. During collision, particles rebound off one another and change velocity directions due to transfers of momentum.

lattice gas automata to lattice Boltzmann method

The idea of only one particle per node is unrealistic since the lattice refinement would have to be at the microscopic scale which goes back to the Hamilton equations and time-expensive computations. The lattice Boltzmann method (LBM) seeks to avoid this refinement by instead describing the number of particles at a particular node as a distribution. Thus, the particle distribution function, n_i(**x**,t), is converted into $f(\mathbf{x}, \mathbf{e}, t)$ where x is the spatial position vector, e is the velocity vector, and t time. The distribution function represents the number of particles of the same mass at time t residing between **x**+d**x** and having velocities between **e**+d**e**.

The collision term referenced in Equation 3 can be considered as the rate of change between the final and initial states of the distribution function. Applying the force (which is the water current in this model) and taking into consideration the collisions between particles, the resulting particle distribution function is as follows.

$$f(x + \mathbf{e}dt, \mathbf{e} + \frac{\mathbf{F}}{m}dt, t + dt)d\mathbf{x}d\mathbf{e} - f(\mathbf{x}, \mathbf{e}, t)d\mathbf{x}d\mathbf{e} = \Omega(f)d\mathbf{x}d\mathbf{e}dt \tag{4}$$

In the next steps the Boltzmann equation and the kinetic form of the particle interactions will be defined. Dividing Equation 4 by $d\boldsymbol{x}d\boldsymbol{e}dt$ and taking the limit of dt as it approaches zero, the particle distribution function with collision can be reduced to

$$\frac{Df}{dt} = \Omega(f) \tag{5}$$

which means the total rate of change of f is proportional to the rate of the collision between particles. Expanding Df into its spatial, velocity, and time components and dividing by dt the result is

$$\frac{Df}{dt} = \frac{\partial f}{\partial \mathbf{x}}\frac{d\mathbf{x}}{dt} + \frac{\partial f}{\partial \mathbf{e}}\frac{d\mathbf{e}}{dt} + \frac{\partial f}{\partial t} \tag{6}$$

where $\frac{dx}{dt}$ represents the velocity $\mathbf{e}$ and $\frac{de}{dt}$ represents acceleration $\mathbf{a}$. The acceleration can be written as force divided by mass which converts the equation into

$$\frac{\partial f}{\partial t} + \frac{\partial f}{\partial x}\mathbf{e} + \frac{\mathbf{F}}{m}\frac{\partial f}{\partial \mathbf{e}} = \Omega(f) \tag{7}$$

Then the Boltzmann equation can be defined for a case where external forces are zero[21]

$$\frac{\partial f}{\partial t} + \mathbf{e} \cdot \bigtriangledown f = \Omega(f). \tag{8}$$

The kinetic form is the same as in the lattice gas automata (Equation 3) discretized into α velocity directions from 1 to M.

$$f_\alpha(\mathbf{x} + \mathbf{e}_\alpha \delta t, t + \delta t) = f_\alpha(x, t) + \Omega_\alpha(x, t)) \tag{9}$$

Lastly, the collision term is most commonly represented by the Bhatnagar-Gross-Krook collision model [39]:

$$\Omega_\alpha = \frac{1}{\lambda}(f_\alpha - f_\alpha^{eq}) \tag{10}$$

where f^{eq} is the equilibrium distribution function and λ is the rate of relaxation. The next subsection will describe the equilibrium distribution function in detail.

Equilibrium distribution function

The fully discretized Boltzmann equation in time (δt) and space ($\delta x = \mathbf{e}_\alpha \delta t$),

$$f_\alpha(x_\alpha + \mathbf{e}_\alpha \delta t, t + \delta t) = f_\alpha(x_\alpha, t) - \frac{\delta t}{\lambda}(f_\alpha - f_\alpha^{eq}), \tag{11}$$

is usually solved in two steps, i.e. streaming and collision, similarly to the lattice gas automata. The particle distribution function can be split into the two steps as follows.

$$\text{collision step: } \bar{f}_\alpha(x_\alpha, t+\delta t) = f_\alpha(x_\alpha, t) - \frac{\delta t}{\lambda}(f_\alpha(x_\alpha, t) - f_\alpha^{eq}(x_\alpha, t)) \tag{12}$$

$$\text{streaming step: } f_\alpha(x_\alpha + e_\alpha \delta t, t+\delta t) = \bar{f}_\alpha(x_\alpha, t+\delta t) \tag{13}$$

During the implementation of the LBM, the collision and streaming steps occur within the same iteration and it is unnecessary to save both $\bar{f}_\alpha(x_\alpha, t+\delta t)$ and $f_\alpha(x_\alpha + e_\alpha \delta t, t+\delta t)$. During the collision step, the particles collide with other particles or with boundaries and relax towards equilibrium. In the streaming step the particles move in the direction of their discretized velocities. The model is set up so that magnitude of the velocity vector is the same as the space discretization, or, in other words, particles only move one node away within one time step.

The equilibrium particle distribution function, f^{eq}, used in the BGK collision step is an expansion of Maxwell's distribution function for low Mach number M [21]. The normalized Maxwell distribution function is

$$f^{eq} = \frac{\rho}{2\pi/3} e^{-\frac{3}{2}(\mathbf{e}-\mathbf{u})^2} = \frac{\rho}{2\pi/3} e^{-\frac{3}{2}(\mathbf{e}\cdot\mathbf{e})} e^{\frac{3}{2}(2\mathbf{e}\cdot\mathbf{u}-\mathbf{u}\cdot\mathbf{u})} \tag{14}$$

where $\mathbf{u}$ is the macroscopic velocity of particles in fluid, $\mathbf{e}$ is the directional velocity vector for each particle, and ρ is the density of particles in the lattice. The Maxwell distribution function can be further expanded for small velocities, $\frac{u}{c_s} << 1$, since the particles are only moving one node away.

$$f^{eq} = \frac{\rho}{2\pi/3} e^{-\frac{3}{2}(\mathbf{e}\cdot\mathbf{u})[1+3(\mathbf{e}\cdot\mathbf{u}-\frac{3}{2}(\mathbf{u}\cdot\mathbf{u}+\frac{9}{2}(\mathbf{e}\cdot\mathbf{u})^2]} \tag{15}$$

The expansion is up to the second order so as to match the accuracy of the Navier-Stokes equation. Finally, the equilibrium distribution function can be explicitly described from the Maxwell distribution function by discretizing into α velocity directions ranging from

1 to n.

$$f_\alpha^{eq} = w_\alpha \rho[1 + \frac{3}{c^2}(\mathbf{e}_\alpha \cdot \mathbf{u}) + \frac{9}{2c^4}(\mathbf{e}_\alpha \cdot \mathbf{u})^2 - \frac{3}{2c^2}\mathbf{u} \cdot \mathbf{u}] \tag{16}$$

where w_α is the weighting factor for each direction, ρ is the total particle density at node (i), c is the speed of sound ($\frac{\delta x}{\delta t} = 1$ usually), and u is the velocity vector [28, 39].

The equilibrium distribution function is used to calculate $\bar{f}_\alpha(x_\alpha, t + \delta t)$ at the end of the collision step:

$$f(t+1) = \lambda f(t) + (1 - \lambda) f^{eq}. \tag{17}$$

The equilibrium distribution is the same for every dimension and space discretization.

LBM to Navier-Stokes

By using Chapman-Enskog theory, the Navier-Stokes equations can be derived from the lattice Boltzmann equation [39]. Rescaling time and space as $t_1 = \epsilon t$, $t_2 = \epsilon^2 t$, and $x_1 = \epsilon x$ with $\frac{\partial}{\partial t} = \epsilon \frac{\partial}{\partial t_1} + \epsilon^2 \frac{\partial}{\partial t_2}$ and $\frac{\partial}{\partial x} = \epsilon \frac{\partial}{\partial x_1}$, the particle distribution function, f_α, can be expanded as

$$f_\alpha = f_\alpha^{(0)} + \epsilon f_\alpha^{(1)} + \epsilon^2 f_\alpha^{(2)} + O(\epsilon^2). \tag{18}$$

The macroscopic quantities of mass and momentum can be determined from the particle distributions f_α by applying Stoke's theorem to the conservation laws [21, 39].

$$\rho(x,t) = m \int f(\mathbf{x}, \mathbf{e}, t) d\mathbf{e} \tag{19}$$

$$\rho(x,t)\mathbf{u}(\mathbf{x},t) = m \int f(\mathbf{x}, \mathbf{e}, t)\mathbf{e}\ d\mathbf{e} \tag{20}$$

where m is the mass of the particles, usually set to 1. The lattice Boltzmann method

is evaluated in discrete time and space, thus, the integration terms can simplified and evaluated as summations.

$$\rho = \sum_{\alpha=0}^{n-1} f_\alpha = \sum_{\alpha=0}^{n-1} f_\alpha^{eq} \tag{21}$$

$$\rho \mathbf{u} = \sum_{\alpha=1}^{n-1} e_\alpha f_\alpha = \sum_{\alpha=1}^{n-1} e_\alpha f_\alpha^{eq} \tag{22}$$

The fluid viscosity in terms of a single relaxation time, λ, can be derived from the BGK collision term for the Boltzmann equation

$$\nu = (\tau - \frac{1}{2}) c_s^2 \tag{23}$$

where the speed of sound in the lattice, c_s^2, is $(\frac{\delta x}{\delta t})/3$ (usually $\frac{\delta x}{\delta t}$ is set to 1).

1.3 Literary Review

The lattice Boltzmann method can be used to solve a variety of systems of differential equations including turbulent fluid flow over complex geometrical boundaries, multicomponent fluid flow over porous material, chemically reacting fluids, particle suspensions in fluids, and others [27,38]. Specifically, Yu et al claims that the lattice Boltzmann simulations of suspensions in a fluid are highly accurate in terms of multiple and single-particle suspensions. In fact, some LBM simulations with single-particle suspensions produced results that had not yet been obtained with physical experiments but were later confirmed correct [27, 38]. In addition, the computational time of the lattice Boltzmann method only linearly increases with the number of suspended particles in the model [13].

This project is a unique application of the lattice Boltzmann method. The aim of this project is to explore the flexibility of the method by varying bathymetric features in the system by analyzing the distribution of two phytoplankton species competing for two nutrients, one preferred, with bottom-boundry mussel consumption in two dimensions.

Modeling the phytoplankton and nutrient interaction in one dimension was performed through a Navier-Stokes system by Mellard[22] and Stojsavljevic[32]. Both projects aimed at determining the vertical distribution of phytoplankton in a one dimensional water column. The effects of mussels at the bottom of the water column was not considered. This model explored how light and nutrients limit the phytoplankton population and influence the population's preferred water depth. An ODE solver was used to find the solution to the convection-diffusion biological system. Mellard's model will be referenced in this project for the biological interactions.

Rowe also studied phytoplankton and mussel interactions using measurements taken from different sections of Lake Michigan [29]. Rowe created geostatistical models in order to estimate the abundance of dressenid mussels covering Lake Michigan. These measurements were compared to satellite sensory observations of the distribution of phytoplankton throughout the lake to make conclusions about the depletion of the natural spring phytoplankton bloom that used to be typical of Lake Michigan.

Fillingham [4] completed his PhD thesis on the effects of dressenid mussels on the spring phytoplankton blooms and near-shore nutrients of Lake Michigan. This model was similar to Mellard's in that it is one dimensional and considers the habitat of different layers of water within the lake. Fillingham utilized historical data of the population counts of Lake Michigan to create a time-lapse simulation of the phytoplankton population. The simulation was carried out by solving a system of differential equations to determine the population total for phytoplankton each year.

Smith et al explored the fluid flow of water, with suspension of phytoplankton, around mussel clusters using the lattice Boltzmann method [30]. Their aim was to find a mussel cluster structure that optimizes the phytoplankton filtration. The exact shape of each mussel was considered when constructing their model and the lattice Boltzmann method proved to be flexible enough to accommodate for the complex geometry of a mussel cluster.

Many others have taken a biological approach to studying the food system of Lake Michigan including Kerfoot [11], Link [17], Nalepa [25], Prins [26], Strayer [33], and Tang [35]. The quagga mussel impact on freshwater lakes and rivers is not isolated to Lake Michigan. The negative impacts of quagga mussels on the aquatic community needs to be better understood in order to take a step forward in creating a solution to the invasion of quagga mussels in all freshwater lakes.

2 Modeling the Aquatic System

2.1 Convection - Diffusion Model

The phytoplankton population and nutrient concentration within Lake Michigan will be implemented as a particle suspension within the fluid. The particle suspensions will interact with one another through consumption of nutrients by the phytoplankton and consumption of phytoplankton and recycling of nutrients by the bottom-boundary quagga mussel population. The biological interactions are described below as a one-dimensional system of differential equations but will be implemented as a two-dimensional system. In essence, the one dimensional model will be expanded to two dimensions by describing the passive movement of the nutrients and phytoplankton by the results of the two-dimensional fluid fluxes of the LBM, the active movement of the phytoplankton will occur only in the vertical dimension, and the growth and consumption rates of phytoplankton and nutrients are calculated for each individual node. The particle suspension will go through the lattice Boltzmann streaming step and a modified collision step.

The system of partial differential equations represent a one-dimensional model of two phytoplankton species, two nutrients, and one mussel species. The phytoplankton populations are competing for light and a preferred nutrient. The nutrients for this model are assumed to be ammonia and nitrate. Ammonia is the preferred nutrient because it is easier for the phytoplankton to consume and it is the more abundant nutrient due to the assumption that quagga mussels recycle ammonia back into the system. This model has

been developed through many literature sources but Mellard's work is referenced most often in this thesis[22].

The mussel population resides at the lowest depth and interacts with the suspended phytoplankton and nutrient system through consumption of phytoplankton and recycling nutrients. The growth of the mussel population at each node is described by a differential equation while the consumption of phytoplankton and consumption of nutrients is described as boundary conditions represented as partial differential equations.

The phytoplankton species are assumed have the ability to actively move by changing their buoyancy in order to find optimal nutrient and light conditions. The passive movement is diffusion flow throughout the fluid space while the growth term is based on nutrient consumption, light availability (I), and natural death or mussel consumption. The phytoplankton's movement can be described as:

$$\begin{cases} \frac{\partial p_1}{\partial t} = -\nu_1 \frac{\partial p_1}{\partial z} + \frac{\partial}{\partial z}(D\frac{\partial p_1}{\partial z}) + G_1(p_1, p_2, N_1, N_2, I) \\ \frac{\partial p_2}{\partial t} = -\nu_2 \frac{\partial p_2}{\partial z} + \frac{\partial}{\partial z}(D\frac{\partial p_2}{\partial z}) + G_2(p_1, p_2, N_1, N_2, I) \\ = \text{[Active Movement]+[Passive Movement]+[Growth/Loss]} \end{cases} \tag{24}$$

where G is dependent on the limiting resource and is reflected in the nutrient growth term, H, below. The velocity component of the active movement, ν, represents the velocity at which the phytoplankton actively move up or down towards the best conditions [22].

The nutrients also go through passive movement by diffusive flow through the fluid space. In addition, nutrients are consumed by the phytoplankton and recycled into the system through deceased phytoplankton biomass.

$$\begin{cases} \frac{\partial N_1}{\partial t} = \frac{\partial D}{\partial z}\frac{\partial N_1}{\partial z} + D\frac{\partial^2 N_1}{\partial z^2} - H_1(p_1, p_2, N_1, N_2, I) + \epsilon l_1 p_1 + \epsilon l_2 p_2 \\ \frac{\partial N_2}{\partial t} = \frac{\partial D}{\partial z}\frac{\partial N_2}{\partial z} + D\frac{\partial^2 N_2}{\partial z^2} - H_2(p_1, p_2, N_1, N_2, I) + \epsilon l_1 p_1 + \epsilon l_2 p_2 \\ = \text{[Passive Movement]-[Uptake by Phytoplankton]+[Recycling from Phytoplankton death]} \end{cases} \tag{25}$$

The consumption and population growth of the quagga mussel population at the bottom of the lattice area is described through a growth and loss term

$$\frac{dM}{dt} = R_M(M, P_1, P_2) = r_{max}M(1 - \frac{M}{M_{max}})(\frac{P_1 + P_2}{\kappa_M + P_1 + P_2}) - qM \tag{26}$$

where r_{max} is the maximum consumption rate, M is the population density at time t, the population carrying capacity in the lake is M_{max}, the half-saturation constant for phytoplankton consumption is κ_M, and q is the loss rate.

Phytoplankton Growth Rate

As stated, the growth terms G and H are dependent on nutrient and light availability which is described by the equations here. The light equation follows the Beer-Lambert law relating the attenuation of phytoplankton to the medium the light is traveling through, i.e. water.

$$I(z,t) = I_0(t)e^{-\int((a_b + a_1P_1(s) + a_2P_2(s))ds, 0, z)} \tag{27}$$

Phytoplankton growth occurs according to Liebig's Law of the Minimum [8, 22], and the growth term, G_i, is dependent on two limiting factors, light and nutrients, where i represents population 1 or 2. The light and nutrient availability for each phytoplankton take the form of Michaelis-Menten enzyme kinetics when it is the limiting resource. The steps for calculating the growth term are as follows.

First, the Michaelis-Menten function for light is calculated where where ρ_{max} represents the maximum growth rate for the associated population and λ_i is the light half-saturation constant.

$$I_i = \rho^i_{max}(\frac{I}{I + \lambda_i}) \tag{28}$$

Next, the nutrient uptake is determined, again using the Michaelis-Menton form. The maximum growth rate is ρ while κ represents the nutrient half-saturation constant of phytoplankton species i for nutrient 1 or 2. A new term, ψ, describes the preference of phytoplankton species i for N1 (ammonia) versus N2 (nitrate).

$$Nut_i = \rho^i_{max}(\frac{N_1}{N_1 + \kappa^i_{N_1}} + \frac{N_2}{N_2 + \kappa^i_{N_2}} e^{-\psi_i N1}) \tag{29}$$

Finally, the phytoplankton population net growth rate, G_i, is calculated using Leibig's Law of the Minimum with a loss rate l_i.

$$G_i = \min(I_i, Nut_i) - l_i \tag{30}$$

The phytoplankton population growth is evaluated at each node throughout the discretized lattice.

Nutrient Consumption Rate

The consumption rate for each nutrient reflects the Nut_i term from the phytoplankton growth calculation. The amount of nutrient i must be isolated from the total consumption of each phytoplankton species by multiplying the growth rate, $\frac{\min(I_1, Nut_1)}{Nut_1}$ by the fraction N_i / (N_i+half saturation constant for P_i and N_i). The consumption rate for nutrient 2 has an added term due to the preference parameter ψ. Finally, the small amount of recycling of phytoplankton biomass, ϵ is added at the end.

$$H_1 = \rho^1_{max} P_1(-\frac{\min(I_1, Nut_1)}{Nut_1} \frac{N_1}{N_1 + \kappa^1_{N_1}}) + \rho^2_{max} P_2(-\frac{\min(I_2, Nut_2)}{Nut_2} \frac{N_1}{N_1 + \kappa^2_{N_1}}) + \epsilon(l_1 P_1 + l_2 P_2) \tag{31}$$

$$H_2 = \rho^1_{max} P_1(-\frac{\min(I_1, Nut_1)}{Nut_1}\frac{N_2}{N_2 + \kappa^1_{N_2}}e^{-\psi_1 N_1}) + \rho^2_{max} P_2(-\frac{\min(I_2, Nut_2)}{Nut_2}\frac{N_2}{N_2 + \kappa^2_{N_2}}e^{-\psi_2 P_1}) + \epsilon(l_1 P_1 + l_2 P_2) \tag{32}$$

The consumption rate of nutrients is evaluated at each node throughout the system.

Active Movement of Phytoplankton

The buoyancy term for the phytoplankton, $-\nu_i \frac{\partial p_i}{\partial z}$, also takes the Michaelis-Menton form of enzyme kinetics and is evaluated only in the vertical dimension. The swimming speed, or buoyancy ability, of the phytoplankton at a specific node is dependent on the gradient of the net growth rate G_i of the nodes directly above or below it, the maximum swimming speed, and the Michaelis constant, K_{swim} [22], representing when the reaction rate is half of the maximum velocity.

$$\nu_i = \nu_{max,i}(\frac{\frac{\partial G_i}{\partial z}}{|\frac{\partial G_i}{\partial z}| + K_{swim}}) \tag{33}$$

This velocity is implemented at the end of the collision step and, within the context of the LBM, represents a distribution of particles from each node either moving up one node or moving down one node towards ideal conditions.

Initial and Boundary Conditions

The initial conditions of the system represent an initial population density at for each node in the lattice area.

$$\begin{cases} P_1(z,0) = P_1^0(z) \\ P_2(z,0) = P_2^0(z) \\ N_1(z,0) = N_1^0(z) \\ N_2(z,0) = N_2^0(z) \\ M(t) = M_0 \end{cases} \tag{34}$$

And the boundary conditions implemented for time $t \geq 0$ describes the interactions of the suspended phytoplankton and nutrient populations with the mussel population at the bottom of the lake.

$$\begin{cases} \frac{\partial P_1}{\partial z}|_{z=0} = 0, \frac{\partial P_2}{\partial z}|_{z=0} = 0, \frac{\partial N_1}{\partial z}|_{z=0} = 0, \frac{\partial N_2}{\partial z}|_{z=0} = 0 \\ \frac{\partial P_1}{\partial z}|_{z=z_d} = -r_{max} M(1 - \frac{M}{M_{max}})(\frac{P_1}{\kappa_M + P_1 + P_2}|_{z=z_d}) \\ \frac{\partial P_2}{\partial z}|_{z=z_d} = -r_{max} M(1 - \frac{M}{M_{max}})(\frac{P_2}{\kappa_M + P_1 + P_2}|_{z=z_d}) \\ \frac{\partial N_1}{\partial z}|_{z=z_d} = \alpha R_M + \beta_r^1 \\ \frac{\partial N_2}{\partial z}|_{z=z_d} = \beta_r^2 \end{cases} \tag{35}$$

where α is the amount of mussel consumption recycled back into the system and β is the concentration of nutrients within the sediment of the lake.

The phytoplankton population growth, nutrient consumption, mussel consumption and recycling, and boundary conditions were implemented in this simulation as the addition of particles or subtraction of particles from the population distributions at each node during the collision step of the lattice Boltzmann model. One trait of the lattice Boltzmann method is that any nonlinear advection, convection, or diffusion terms can be avoided

and implemented during a streaming step.

2.2 Biological Parameters

Table 1 lists the parameters used for the model, the units for each parameter, and the description in reference to this biological model. The two phytoplankton species are assumed to be statistically similar in their growth, loss, and active movement parameters. Phytoplankton 1 has a higher light half-saturation constant ($\lambda_1 > \lambda_2$) while phytoplankton 2 has a higher nutrient half-saturation constant ($\kappa_1 < \kappa_2$). This translates to P1 needing more light than P2, and P2 needing more nutrients than P1. This preference should be reflected in the results.

Nutrient 1 is assumed to represent ammonia while nutrient 2 is representing Nitrate. As stated earlier, ammonia is the preferred nutrient due to its easier absorption by the phytoplankton. In addition, the quagga mussel only produces ammonia as a waste product so there are higher concentrations of nutrient 1 in the system.

There are many species of phytoplankton, types of nutrients, and species of mussels that could be used as reference for the biological interactions. The specific parameters for this model are based on common species or types found in Lake Michigan.

Cyanobacteria (blue-green algae), green algae, diatoms, and flagellates are just a few of the types of phytoplankton found naturally within Lake Michigan. Measurements of Lake Michigan were collected by the Division of Water Supply and Pollution Control [15] from stations ranging 1 to 10 miles of the shore. Phytoplankton was occured in ranges from 1000 - 5000 total species counts per milliliter while the type of species found were Melosira, Cyclotella, and Stephanodiscus near the shore and Asterionella, Tabellaria, Fragilaria, and Synedra in the middle of the lake. The most highly concentrated species are Melosira and Cyclotella which will be the two species used in this thesis. The report also stated that light penetrated into Lake Michigan about 2 meters to 12 meters but was usually more than 6 meters deep.

The quagga mussel, or *Dreissena bugensis*, is the specific mussel of interest for this project. The National Oceanic and Atmospheric Association found that this mussel can be concentrated at 35,000 mussels per square meter along the bottom of Lake Michigan [23].

The National Service Center for Environmental Publications[15] and the DNR of Wisconsin [6] reports on the concentration levels of ammonium, nitrate, and other nutrients found in Lake Michigan. The half saturation constants for ammonium and nitrate in phytoplankton are reported several publications and summarized in Table 1 [2, 16, 34].

3 Model Implementation

3.1 Lattice Boltzmann Discretization and Boundary Conditions

This project primarily utilizes the two dimensional - nine velocity square lattice arrangement (D2Q9). Other commonly used discretizations include one dimensional-three velocity (D1Q3) and three dimensional - 27 velocities (D3Q27). The following sections describe each lattice arrangement and list the directional velocity vectors and weighting factors which are used in the equilibrium distribution function, Equation 16. The weighting factors are established in the publications by He and Luo [10], Qian [28], and Yu [39]. One benefit of the lattice Boltzmann method is that the equilibrium distribution function does not vary from one lattice arrangement to the next. Instead, only the velocity directional vectors and the weighting factors are updated to reflect the lattice arrangement being used.

D1Q3 Weights and Velocities

The one dimensional lattice Boltzmann model consists of three velocities, e_+, e_-, and e_0. Consider the one-dimensional water column. Each lattice node represents location e_0 in Figure 3.1 with particle distribution *f*. The proportion of particles moving up one node has the velocity e_+ while the proportion of particles moving down has the velocity e_-.

A downward current would be represented by a larger proportion of particles moving in the e_- direction.

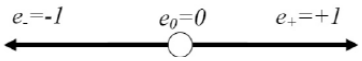

Figure 3.1: D1Q3 velocity directions

The mass density for each lattice node is represented as $f_1 + f_2 + f_3 = fe_\alpha$. The weighting factors are normalized such that $\sum w_\alpha = 1$ and are defined as $w_0 = \frac{2}{3}$ and $w_{1,2} = \frac{1}{6}$ [28]. This translates to $\frac{2}{3}$ of the particles having no velocity, $\frac{1}{6}$ streaming up, and $\frac{1}{6}$ streaming down.

D2Q9 Weights and Velocities

The two dimensional model has nine velocity vectors: the 4 nearest neighbors, the 4 next-nearest (or 90 degree angled) neighbors, and the center non-moving node.

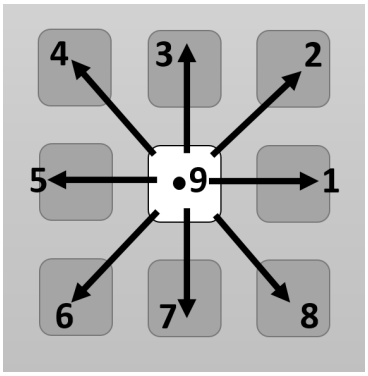

Figure 3.2: D2Q9 velocity directions (α labeled at each node).

The same discretized equilibrium equation (16) is applied to every discretization and dimension. The velocity and weighting factors in the direction of α for the D2Q9 model are listed below [28, 39].

$$e_\alpha = \begin{cases} (0,0) & \alpha = 0 \\ c(\cos((\alpha-1)\frac{\pi}{4}), \sin((\alpha-1)\frac{\pi}{4})) & \alpha = 1,3,5,7 \\ \sqrt{2}c(\cos((\alpha-1)\frac{\pi}{4}), \sin((\alpha-1)\frac{\pi}{4})) & \alpha = 2,4,6,8 \end{cases} \tag{36}$$

$$w_\alpha = \begin{cases} \frac{4}{9} & \alpha = 9 \\ \frac{1}{9} & \alpha = 1,3,5,7 \\ \frac{1}{36} & \alpha = 2,4,6,8 \end{cases} \tag{37}$$

D3Q27 Weights and Velocities

One example of a three dimensional lattice arrangement is with 27 velocity directions which can be visualized in the cube below.

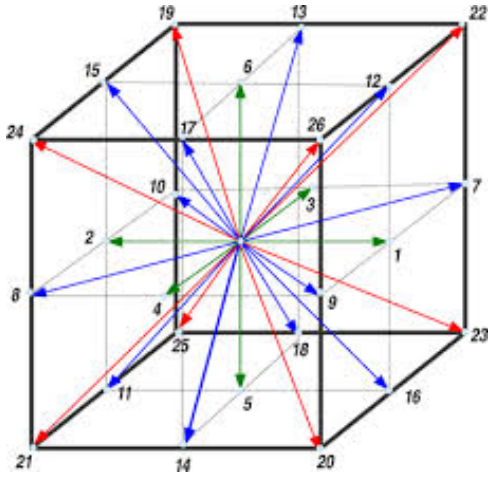

Figure 3.3: D3Q27 velocity directions.

He and Luo [10] explicitly explore the three dimensional expansion of the D2Q9 model. The equilibrium particle distribution function is unchanged while the particle velocities and weighting factors are determined as:

$$e_\alpha = \begin{cases} (0,0,0) & \alpha = 0 \\ (\pm1,0,0)c, (0,\pm1,0)c, (0,0,\pm1)c & \alpha = 1,2,...,6 \\ (\pm1,\pm1,0)c, (\pm1,0,\pm1)c, (0,\pm1,\pm1)c & \alpha = 7,8,...,18 \\ (\pm1,\pm1,\pm1)c & \alpha = 19,20,...,26 \end{cases} \tag{38}$$

$$w_\alpha = \begin{cases} \frac{8}{27} & \alpha = 0 \\ \frac{2}{27} & \alpha = 1, 2, ..., 6 \\ \frac{1}{54} & \alpha = 7, 8, ..., 18 \\ \frac{1}{216} & \alpha = 19, 20, ..., 26 \end{cases} \tag{39}$$

While the implementation of a three-dimensional model will have more components, one can see that it is still a standard expansion of the one-dimensional LBM model.

Boundary Conditions

The boundary conditions of the lattice Boltzmann method usually include a type of inflow/outflow boundary and a bounceback boundary.

The inflow boundary used in this project was an added amount of particles being added to the left side of the two-dimensional area and the same amount of particles taken out of the area on the right side. Thus, a literal current was replicated in the model. Another type of inflow-outflow method is a periodic boundary condition such that any particles streaming out the left (right) side of the lattice area then is cycled back to the right (left) side. This flow functions as a closed system.

The simulation of particles rebounding off of solid boundaries can be implemented in a variety of ways. First, consider the full-way no-slip bounceback. After the boundary nodes are identified within the simulation area, the full-way no-slip bounceback occurs by reversing the velocity of any particle that streams into a boundary node [38]. Figure 3.4 shows an example of two particles streaming into a boundary node.

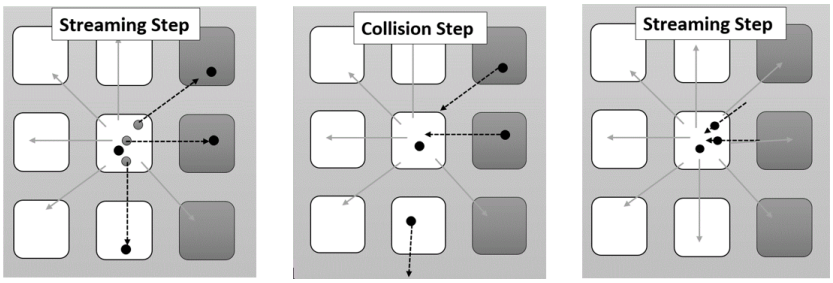

Figure 3.4: Example of streaming into a boundary node. During collision step, reverse the velocity.

The figure shows that it takes a full iteration (collision and streaming step) for particles to exit the boundary nodes. One drawback of this condition is that the boundary for the full-way bounceback cannot be a smooth curve. Instead, a curve can be created by stair-stepping along the node boundaries. When necessary, it would be most accurate to have a round boundary described as an actual curve but that introduces difficulties in implementing the model. Thus, in order to take advantage of the simplicity of the LBM, a full-way bounceback off of stair-step shaped boundary scenarios are used the majority of the time. Per Gallivan et al[5], when implementing this type of collision, the full-way bounceback accounts for less than one percent of the computation time.

To represent curved boundaries in a more accurate way, a half-way bounceback method can be used. The half-way bounceback assumes the boundary lies between two nodes and is shown to have second-order accuracy for straight and curved walls. This method will increase the computational time but will also increase the accuracy. The idea is that if a particle starts streaming towards a boundary node, it will recognize the boundary mid-stream and reverse velocity. Thus, the bounceback occurs within one-half iteration instead of a full iteration like for the full-way bounceback. This boundary condition is ideal for circular or smoothly curved boundary conditions [38,39].

Gallivan et al also explored the difference in errors between implementing the full-way bounceback and the half-way bounceback around a circular-cylinder boundary. For both collision types, the root mean square velocity error is less than two percent. In order to fully utilize the short computation time and the flexibility of the lattice Boltzmann method, this project will use the full bounce-back no-slip boundary condition.

3.2 LBM Fluid Flow

This project concentrated on using the two-dimensional, nine-directional LBM model. The one- dimensional model was inaccurate when it came to modeling the real-world fluid flow system due to the lack of collisions between fluid particles. Due to the lack of

particle collisions, the phytoplankton and nutrients in the LBM one-dimensional model did not move as was observed in previous work with Navier-Stokes systems [22].

One advantage of the lattice Boltzmann method is that it is easily expanded into a three dimensional model. The following section will describe a model with 9 velocity directions but the same ideas would apply to other dimensions. As a note, there are a variety of lattice Boltzmann models available online and this project used the D2Q9 fluid flow model created by Haslam [9] as a reference for building the model in Matlab.

The basic outline of the LBM algorithm is as follows:

1. Initialize water matrix (f)
2. Stream
3. Relax towards equilibrium (f^{eq})
4. Collide and Rebound off Boundaries
5. Go back to step 2 and repeat

The space is discretized into a two dimensional space of x-nodes (width) and z-nodes (depth) with x-nodes increasing left-to-right and z-nodes increasing from top to bottom. Due to the LBM relying on geometric shape for the bounceback collisions and boundary conditions, careful set up of the model is necessary. The lattice size was chosen as x=100 and z=100 due to this area being able to adequately fit the bathymetric feature in question and to provide enough area for particle collisions and an accurate fluid flow.

The LBM method is first applied to the fluid flow in the two-dimensional area. Each node has an initial fluid particle density that is evenly split across the nine velocity directions of the model. Thus, the entire fluid matrix is x by z by 9 and the total particles at each node in the two-dimensional area is the summation across the 9 velocity dimensions.

The boundary conditions are then established and the location of each one is stored in vector form to be used later on for the bounce-back collision.

Before entering the iteration loop, the first streaming step occurs. Each of the nine dimensions of the fluid matrix x by z matrices shift according to the direction they represent (Figure 3.2). The ninth dimension is the stationary dimension so no streaming occurs. The inflow and outflow boundaries are implemented such that a particle density is added to the left side and subtracted from the right, for an left to right current.

After the initial streaming, the iteration loop begins. First the particles that moved into a boundary node are saved for bounce-back. Next, the collision or relaxation towards equilibrium occurs (16). The standard weights (37) for equilibrium distribution of D2Q9 LBM are used with the Batnagar Gross Krook collision term. The velocity, u, is effectively calculated by finding the change in particle density. The density, ρ, is the summation of particles over all nine velocity directions.

The terms that were saved for the bounceback collision are now added back into the model at the same node but with the opposite direction. After the collision step with bounceback, streaming occurs again and the loop is complete. The collision - stream loop continues until most of the fluid particles have relaxed into a general fluid flow through the area.

3.3 Biological Simulation

As stated previously, the phytoplankton population and nutrients are being treated as suspended particles within the fluid. The phytoplankton and nutrient populations will go through the same streaming step as the fluid in the algorithm above but will not go through the same collision step. Instead of the collision step, the biological populations will be interacting with one another as described by the biological system above. The light and mussels are treated as a type of boundary condition and so do not act as a particle distribution that goes through the lattice Boltzmann algorithm. An approximate outline of the biological algorithm is:

1. Initialize phytoplankton and nutrient matrices

2. Initial streaming step

3. **Collide**

    - Phytoplankton population change (G_i)
    - Nutrient consumption by phytoplankton (H_i)
    - Mussel boundary consumption and recycling
    - Active Movement by Phytoplankton
    - Calculate proportion of fluid particle distribution (ρ) that was split in each direction, α, and redistribute the same proportion in each direction for the phytoplankton and nutrients

4. **Stream** (Diffusion)

5. Go back to step 3 and repeat

An initial biomass density for P1, P2, N1, N2 at each node is assigned then split evenly among the nine velocity directions. Each component goes through the streaming in the same way as the fluid LBM model. Only the fluid goes through the collision and relaxation step. The collision process for the phytoplankton and nutrients is as follows. Light penetration at each node is calculated using the trapezoidal rule and is affected by the shading from phytoplankton and nutrient concentrations. Next, the mussel consumption occurs which diminishes the phytoplankton population at the bottom of the lake but actually increases the concentration of nutrients in the form of waste. Finally, G and H can be determined.

As stated in the previous section, the growth of the phytoplankton population is limited by light and nutrient availability. The Michaelis-Menten function for light and nutrients are calculated by Equations 28 and 29. Then, the net growth of the phytoplankton population and the consumption of the nutrients are calculated with Equations 30, 31, and 32.

The buoyancy ability, or active movement, of the phytoplankton is determined last by Equation 33. The vertical growth gradient ($\frac{\partial G}{\partial z}$) for the phytoplankton is determined from the next-nearest neighboring nodes. In other words, the gradient for node i is the difference between vertical nodes *i-1* and *i+1*. Once ν is found for both phytoplankton populations, then the movement is represented as a distribution of particles moving up or down from each node moves towards the maximum gradient in its column. Thus, the buoyancy effect is simulated as phytoplankton moving to the area with the best combination of nutrients and light available.

The growth and death of phytoplankton and nutrients have now been established but the collision of particles with one another and the system boundaries need to be implemented. The bounce-back collisions are simulated by determining the proportion of fluid particles that traveled in each direction from each specific node in the lattice. Then, the same proportion of P1, P2, N1, N2 at each node are sent in the corresponding velocity direction. Thus, the suspension of particles in the fluid LBM model has been represented.

3.4 Boundary Conditions

There are four shapes of boundary conditions used for this project; open channel, small hill (Figure 3.5c), large plateau (Figure 3.5b), and steep drop-off (Figure 3.5d). The large plateau boundary condition is of special interest since the Mid-Lake High Plateau is located in Lake Michigan directly east of Milwaukee [23]. The ease in which a variety of boundary conditions can be imposed on the lattice Boltzmann model displays the versatility of the method.

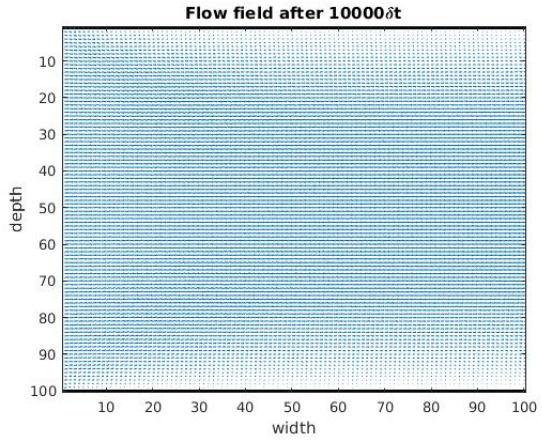

(a) Open channel bound and fluid flow.

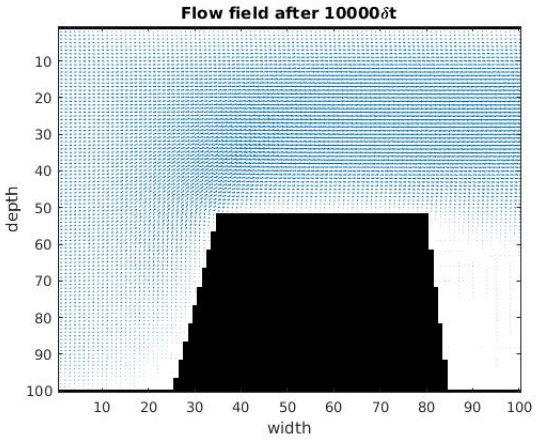

(b) Plateau Bound Fluid Flow.

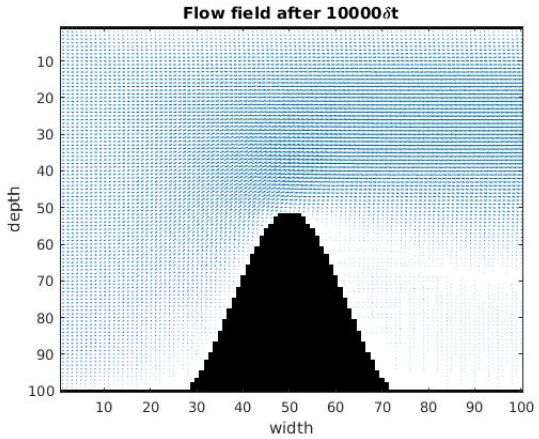

(c) Sinusoidal Hill Bound and Fluid Flow.

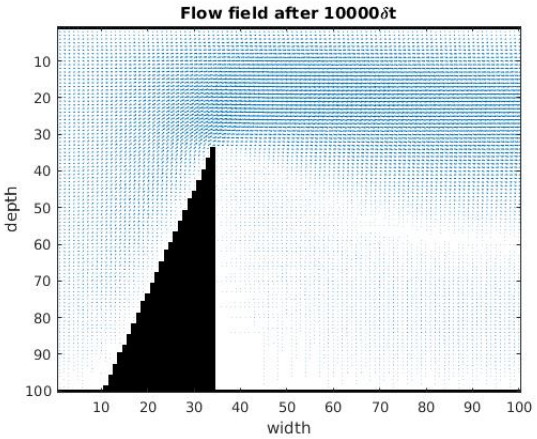

(d) Steep drop off bound and fluid flow.

The left-to-right current is generated by evenly adding an inflow of particles, δ_U, to each node in the left-most column at each time step while also subtracting the same amount of particles from the right-most column at each time step. If the subtraction of particles results in a negative particle distribution within a node, the distribution is set to zero. This addition and subtraction was implemented during the streaming step.

In addition to the solid boundaries, there is a 1-node layer of mussels at the bottom of the lake. This layer extends up and over each boundary condition imposed on the lake floor.

4 Analysis

4.1 Parameters and Assumptions

The reference parameters for the fluid flow, phytoplankton, nutrients, mussels, and light are listed in the tables below. Most parameters have units of day, counts, and mL but the light parameters have a time unit of seconds and the mussel parameters have units of meter squared which cancels out within the subsequent equations. There are ranges for some values due to variability of the real world values found in Lake Michigan. The value listed first is the value used for all simulations unless otherwise specified.

Biomass Parameters			
Parameter	**Value**	**Unit**	**Interpretation**
λ	0.6 (0-1)	-	relaxation rate of equilibrium
dp1	300 (42 - 1876)	$\frac{cells}{mL}$	initial density for Cyclotella
dp2	300 (0-300)	$\frac{cells}{mL}$	initial density for Melosira
dn1	25	$\frac{\mu grams}{mL}$	initial density for Ammonia[6]
dn2	25	$\frac{\mu grams}{mL}$	initial density for Nitrate
$\nu_{(1,2),max}$	0.1	m/day	swimming speed[22]
K_{swim}	.001	1/(m day)	Klausmeier constant[22]
$\kappa^1_{N_{1,2}}$	1	$\frac{\mu mol}{mL}$	nutrient half saturation constant for 1
$\kappa^2_{N_{1,2}}$	100	$\frac{\mu - gramsP}{mL}$	nutrient half saturation constant for P2
$p_{1,max}$	0.04	$\frac{count}{day}$	maximum growth rate P1
$p_{2,max}$	0.04	$\frac{count}{day}$	maximum growth rate P2
$\psi_{1,2}$	0	-	preference parameter of N1
$l_{1,2}$	0.0035	1/day	loss rate for P1 and P2[19,40]
ϵ	0.0005 (0-1)	-	Recycling coefficient[22]
δ_U	0.00001	-	Inflow/Outflow rate
$\delta_{P,N}$	0.000001	-	Inflow/Outflow rate
Mussel Parameters			
dM	5000	$\frac{mussel}{m^2}$	initial density for mussels on bottom
r_{max}	1 (.35-1.42)	1/day	mussel growth rate[17]
M_{max}	35,000	$1/m^2$	mussel carrying capacity[22]
α	0.0006 (0-1)	-	Percent consumption returned to system by mussel
β_{1R}	100 (0-1000)	$\frac{\mu gram}{mL}$	sediment concentration of N1
β_{2R}	100 (0-1000)	$\frac{\mu gram}{mL}$	sediment concentration of N2
q	0	1/day	death rate for quagga mussels
Light Parameters			
I_0	1400	$\frac{\mu molphotons}{m^2 s}$	initial light penetration[22]
a_{bg}	0.35 (0.01 – 10)	1/m	background attenuation coefficient[22]

Biomass Parameters			
Parameter	**Value**	**Unit**	**Interpretation**
$a_{1,2}$	1e-5	$\frac{cellsmL^{-1}}{m}$	algal attenuation coefficient
λ_1	50	$\frac{\mu molphotos}{m^2 s}$	light half-saturation constants[22]
λ_2	5	$\frac{\mu molphotos}{m^2 s}$	light half-saturation constants[22]

Table 1: Biomass, Mussel, and Light Parameters

4.2 Sensitivity Analysis

The rate of relaxation for the particle distribution, λ, cannot be zero or else the particles continue to rebound off each other and the model does not find an equilibrium. A small relaxation rate (0.1) requires more iterations before an equilibrium occurs while a relaxation rate of 1 uses only the equilibrium distribution and there isn't enough collisions to accurately represent fluid flow. A value in the middle (0.6) was chosen as the base parameter.

The light parameters also greatly influence the results of the model. Without deep light penetration, the light becomes the limiting resource and the phytoplankton must concentrate at the towards the surface which inhibits population growth. The background attenuation coefficient,a_{bg}, has a range of 0.01 to 10. When at 0.01, the initial light penetration is not restricted and the light penetrates to nearly the bottom of the lake whereas at a value of 10, the light barely penetrates past the first meter of water. Due to the sensitivity of the simulation to the value of a_{bg}, a value between 0.35 and 0.3 was used which equates to a light penetration of around 10-20m which was the current depth penetration into Lake Michigan per Water Supply and Pollution Control report [15] and the Lake Access report [14].

The sediment parameters, $\beta_{1,2}$, dictate the availability of a nutrient in the sediment of the lake. When β_1 is 0, there is no concentration of ammonia within the sediment and the only source of replenishment of ammonia concentration into the system is from the recycling of the quagga mussels. The recycling of ammonia by the quagga mussels is not high enough to sustain the phytoplankton populations. Similarly, when β_2 is zero, there

is no nitrate in the sediment and there is no replenishment back into the system because nitrate is not a waste product of the mussel. A lack of nutrients in the system results in greatly inhibited or negligent populations of phytoplankton. In each simulation, it was assumed that the same amount of ammonia and nitrate is available in the sediment.

The recycling coefficient introduced by Mellard [22], ϵ, dictates how much of the biomass from the population of phytoplankton is converted into nutrients. For the simulations in this report, epsilon was set to zero in order to better examine the effects of the bottom boundary conditions.

4.3 Bathymetry Influence

The simulation began with fluid, phytoplankton, and nutrient particles being evenly distributed throughout the 100 by 100 lattice space. After cycling through the 'stream and collide' iteration loop around 10,000 times, the system reaches an equilibrium. The fluid equilibrium fluxes are pictured in Figures 3.5a - 3.5d. The distributions of each phytoplankton species and each nutrient are analyzed in the images below.

For each boundary, there is a layer of mussels along the bottom. The following figures show how the phytoplankton population changes its distribution and concentrations depending on the fluid fluxes generated by the bottom features of the lake and the limiting environmental components (nutrients and light). The preferred depths for the phytoplankton species is summarized at the end of the section in Table 2.

First consider the open channel boundary with a depth of 100 meters, Figure 4.6.

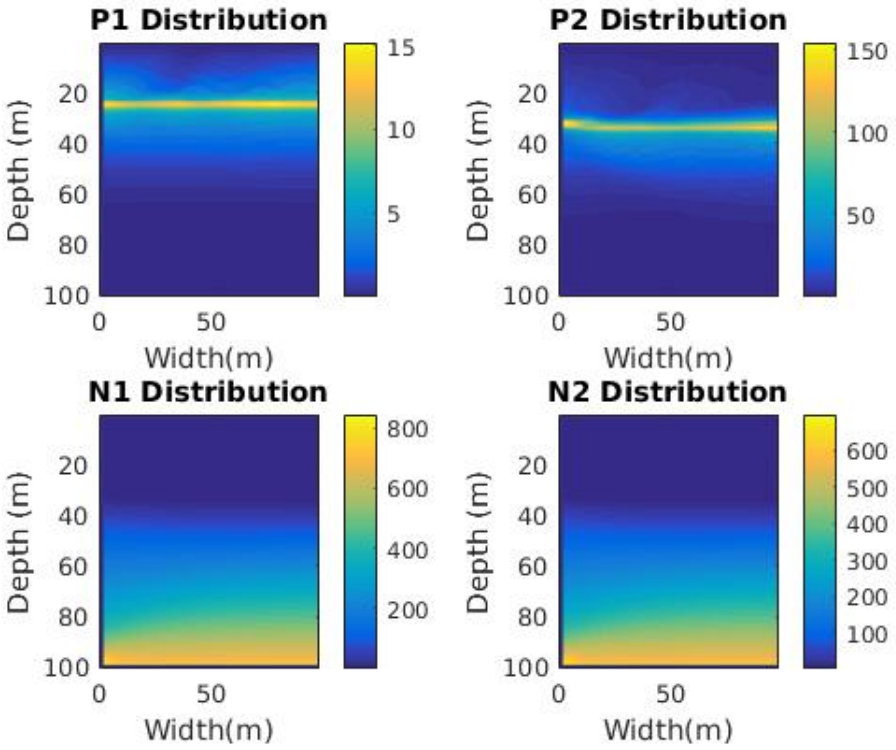

Figure 4.6: Two dimensional distribution of phytoplankton and nutrients in an open channel after 10,000 iterations.

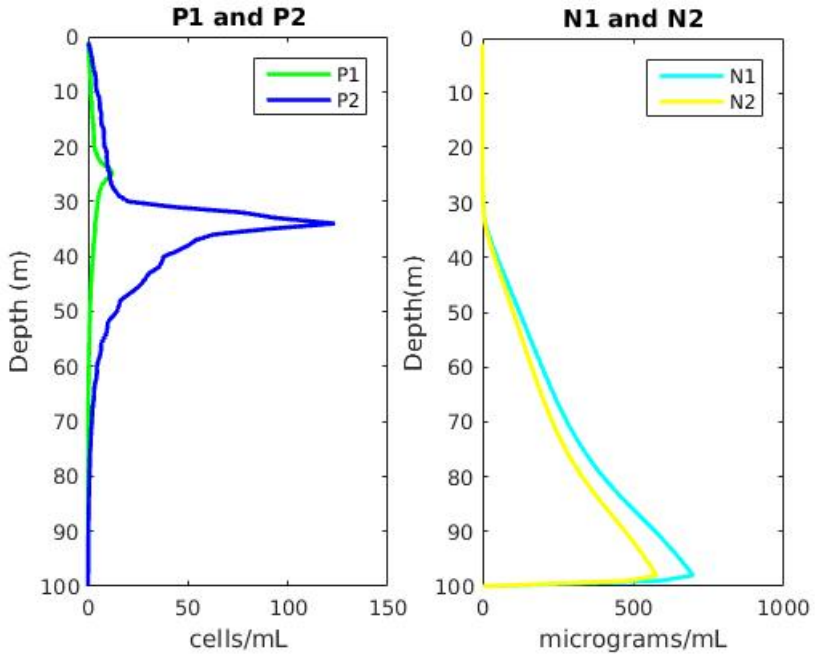

Figure 4.7: One dimensional distribution of phytoplankton and nutrients in an open channel at x=30.

The figures above show phytoplankton 1 preferring a depth of 25 meters while phyto-

plankton 2 prefers a lower depth of 33 meters. In addition, there is a small proportion of phytoplankton 1's population drifting north and south about 10 meters while phytoplankton 2 has a proportion of its population drifting down to about 60 meters in depth. Recall that phytoplankton 1 requires more light than phytoplankton 2 due to the assumption that $\lambda_1 > \lambda_2$. From this assumption it follows that phytoplankton 1 would prefer a shallower depth than phytoplankton 2.

The preferred depth of phytoplankton 2 is directly associated with the depth at which the nutrient availability approaches zero. The nutrients are highly concentrated at the bottom of the water due to the sediment. In addition, nutrient 1 has a higher concentration than nutrient 2 which is most likely due to the recycling of nutrient 1 performed by the mussel population.

Next, the simulation of the Mid-Lake Plateau was considered. The results are pictured below and recorded in the table.

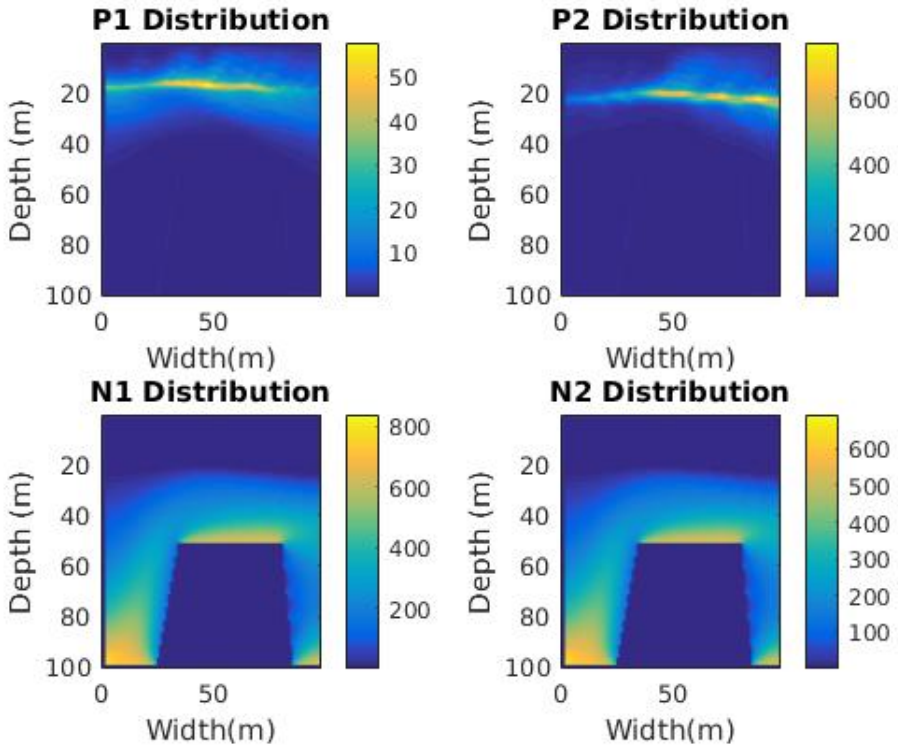

Figure 4.8: Plateau bound results for the two dimensional distribution of phytoplankton and nutrients after 10,000 iterations in normal current.

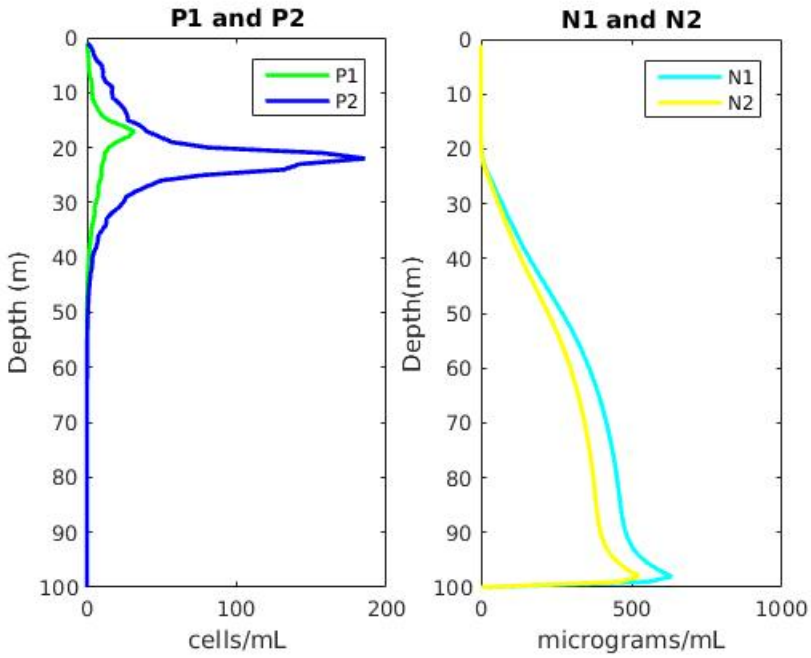

Figure 4.9: 1D Concentrations of P1, P2, N1, and N2 with a plateau bound at x=30 in normal current.

For the plateau bound, phytoplankton 1 prefers to concentrate between 17 and 19 meters in depth while phytoplankton 2 is a little deeper at 21-23 meters. Once again, phytoplankton 2's highest concentration corresponds to the depth at which the nutrient levels approach zero. Similarly to the open channel, phytoplankton 2 has a higher concentration than phytoplankton 1 and nutrient 1 is higher concentrated than nutrient 2.

One difference between the phytoplankton distributions in the plateau bound versus the open bound is the dispersion of a small portion of the phytoplankton population away from the preferred depth. At a width of 40 meters, both of the phytoplankton species start to drift north towards the surface. Comparing this to the flow distribution in Figure 3.5b, there is a high concentration of fluid particles where the water is forced together in order to flow over the boundary. This change in the fluid flux not only caused more dispersion of the phytoplankton populations north and south but also caused the populations to concentrate in a curve instead of a straight line like in the open channel.

The third boundary considered was the rounded hill. The basic flow field for the water shows a curved motion up and over the hill (Figure 3.5c) with water particles being

pushed together in the rectangular area of x=50 to 100 meters and z=10 to 50 meters.

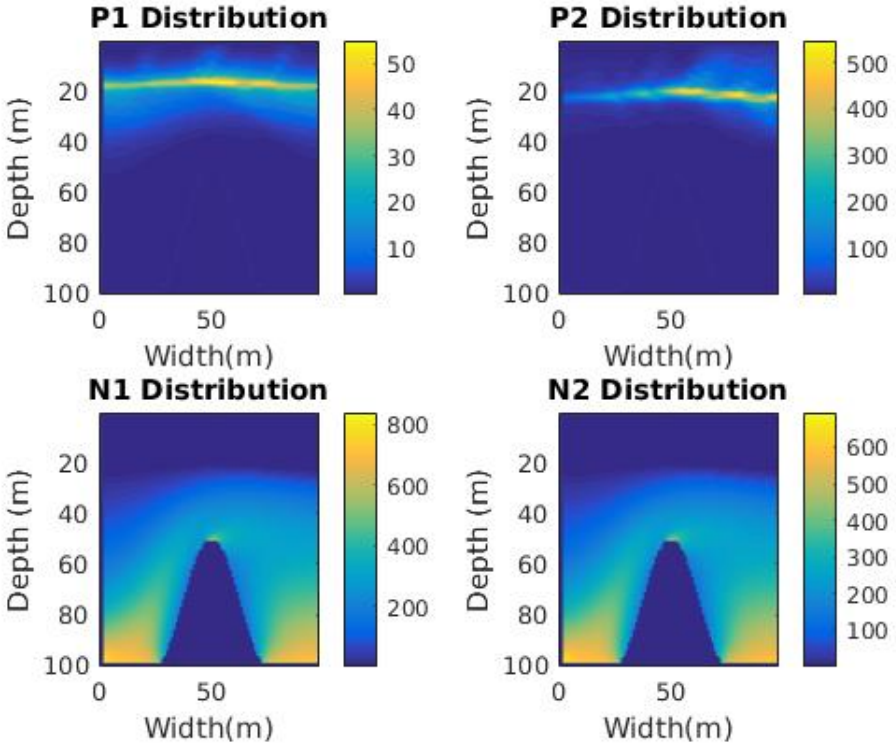

Figure 4.10: Small hill results for the two dimensional distribution of phytoplankton and nutrients after 10,000 iterations.

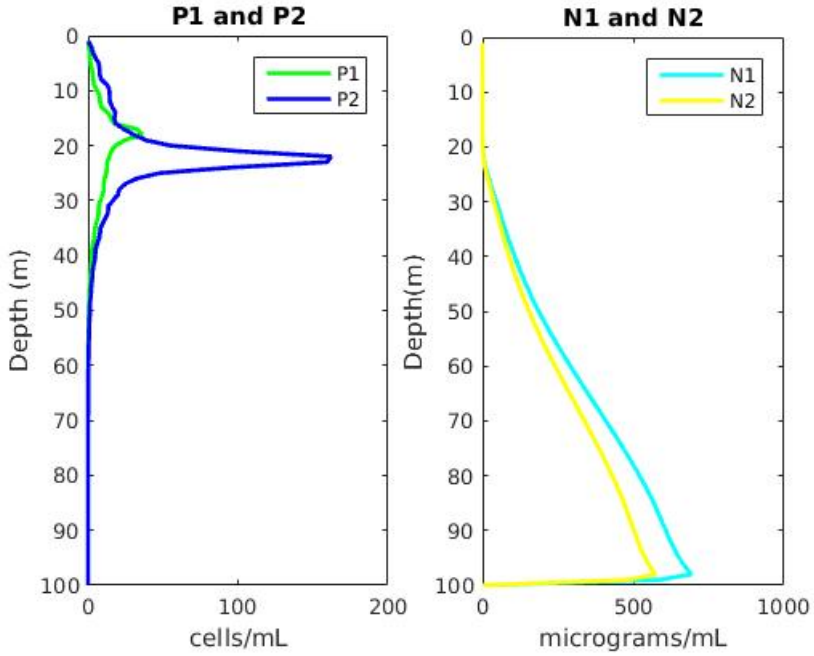

Figure 4.11: 1D Concentrations of P1, P2, N1, and N2 with a small hill bound at x=30 in normal current.

Similarly to the plateau boundary condition, phytoplankton 1 is located at around 17-19 meters in depth while phytoplankton 2 is located at between 21-23 meters. Again, probably due to the fluid fluxes generated around the boundary, the phytoplankton populations have a dispersion effect towards the surface. Also, nutrient 1 and phytoplankton 2 are higher concentrated than nutrient 2 and phytoplankton 1, respectively.

Another difference to note between systems with a hill-type boundary and the open channel is that the phytoplankton populations have a change in concentration across the width of the area which occurs in the plateau simulations as well. In Figure 4.10, both phytoplankton species have a higher concentration between x=40 and x=60 meters which corresponds to the tallest point of the hill. The sediment of the lake provides an inflow of nutrients into the system. It follows logic that the phytoplankton species would concentrate in the areas where nutrients are most abundant which, for those boundaries with a hill-feature, would be directly above the tallest point of the hill.

The final boundary considered for this thesis is the steep drop-off. The steep bound produced interesting fluid fluxes as can be seen in Figure 3.5d. Fluid particles are being pushed together in the area directly to the right of the top of the hill, between x=40-100 meters and z=10-30 meters, while also creating a narrow, curved area with an absence of particles extending from the top of the drop off to the right edge at z=60 meters.

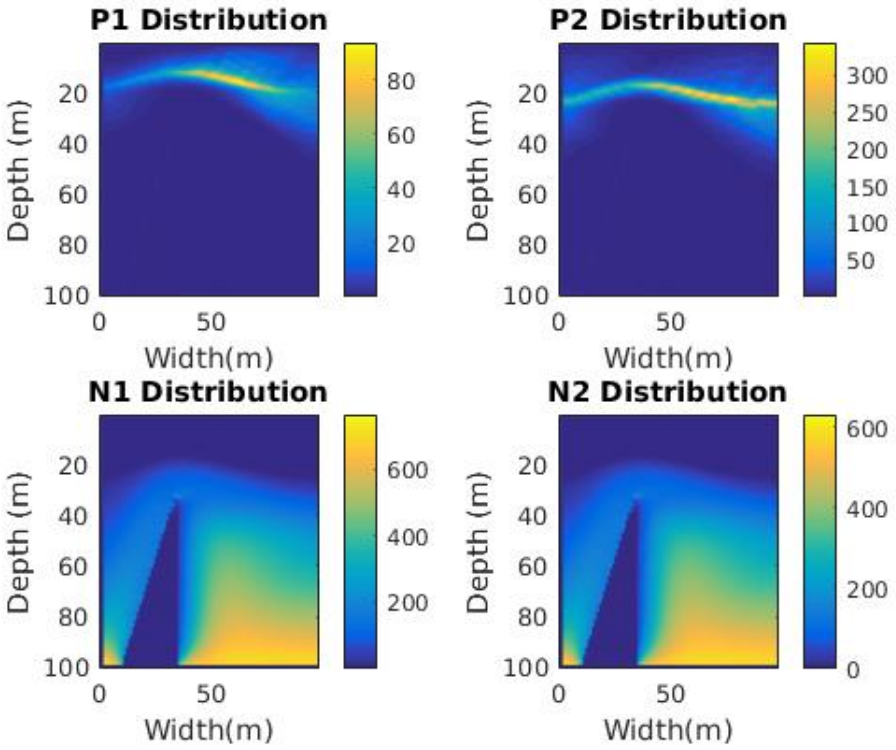

Figure 4.12: Drop-off boundary results for the two dimensional distribution of phytoplankton and nutrients after 10,000 iterations.

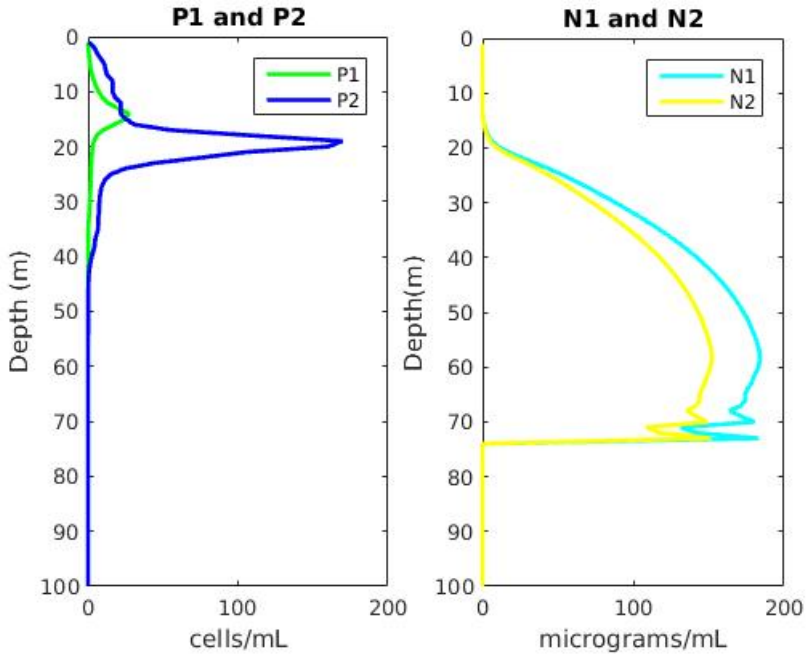

Figure 4.13: 1D Concentrations of P1, P2, N1, and N2 with a steep drop-off bound at x=30 in normal current.

The preferred depth of the phytoplankton concentration was closer to the surface than

previous boundaries and took a steeper curved shape due to the fluid flux up and over the bound. Phytoplankton 1 preferred a depth of 18 meters on the left and right edges of the area while reaching a height of 13 meters directly over the tallest point of the bound. Phytoplankton 2 followed the same trend but at a lower depths of 27 meters at the left and right edges and 19 meters over the bound. Again, dispersion of a small proportion of the phytoplankton population towards the surface of the lake occurs after the top of the hill while dispersion towards the bottom of the lake occurs about 40 meters after the hill. The changes in concentration across the width of the area becomes quite apparent with phytoplankton 1 concentrating between x=45-70 meters and phytoplankton 2 concentrating between x=50-95 meters.

An interesting effect to note is that the curve showing the highest concentration of both phytoplankton species is quite smooth with the drop-off bound. The plateau and the small hill both have curved shapes for the concentration of phytoplankton species as well but the curve is not as smooth as the images in the top row of Figure 4.12. The smoothness of the curve is most likely due to the heightened fluid fluxes generated by the very steep boundary condition.

The following table summarizes the ranges of the preferred depths for each phytoplankton species and each bound.

Boundary Condition	Preferred Depth P1	Preferred Depth P2
Open Channel	25	33
Plateau	17-19	21-23
Hill	17-19	20-22
Steep Drop off	13-20	19-24

Table 2: Locations of preferred depth for each phytoplankton species based on the bottom boundary condition, after 10,000 iterations.

4.4 Scenario: Slow Current

The effects of a slow current in a deep lake are explored in this section by setting δ_U and $\delta_{P,N}$ to 0.0000001. This means very few particles are being added or taken away from the system. The following figures display the effects the slow current has on the phytoplankton and nutrient distributions. No other parameters were altered.

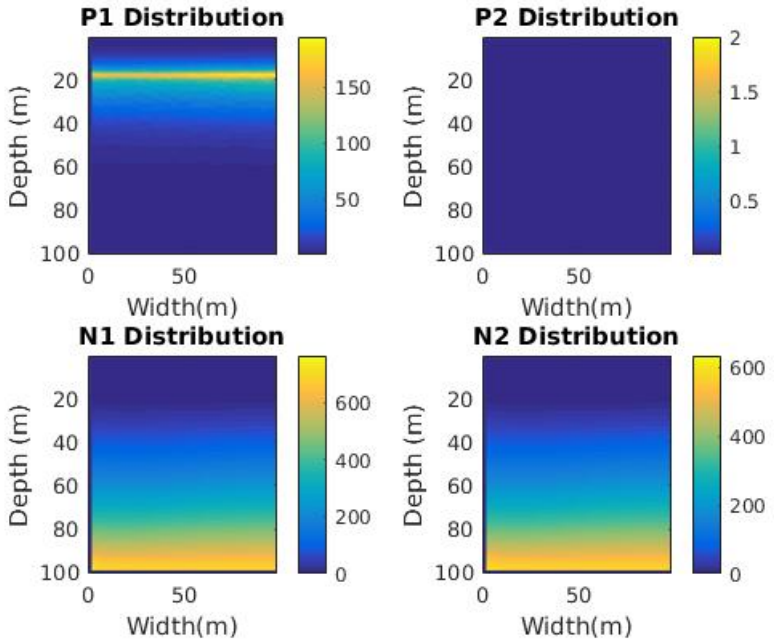

Figure 4.14: 2D population distributions in a slow current with an open channel bound.

An apparent difference between the distributions of the phytoplankton populations with a fast current versus a slow current is the lack of a curved concentration at their preferred depth. Due to the slow current, the fluid fluxes up and over the boundaries are much smaller. Due to the smaller fluid fluxes, there is a diminished build up of fluid particles as the fluid moves through each space which results in fluid flows around boundaries being quite similar to the that in an open channel. In addition to the lack of a curved concentration of phytoplankton, the preferred depth for both species do not vary in depth from one boundary to the next. Phytoplankton 1 prefers a depth of about 19 meters and phytoplankton 2 prefers a depth of about 24 meters.

Looking at Figure 4.13, phytoplankton 2 was not able to survive in the slow current. This

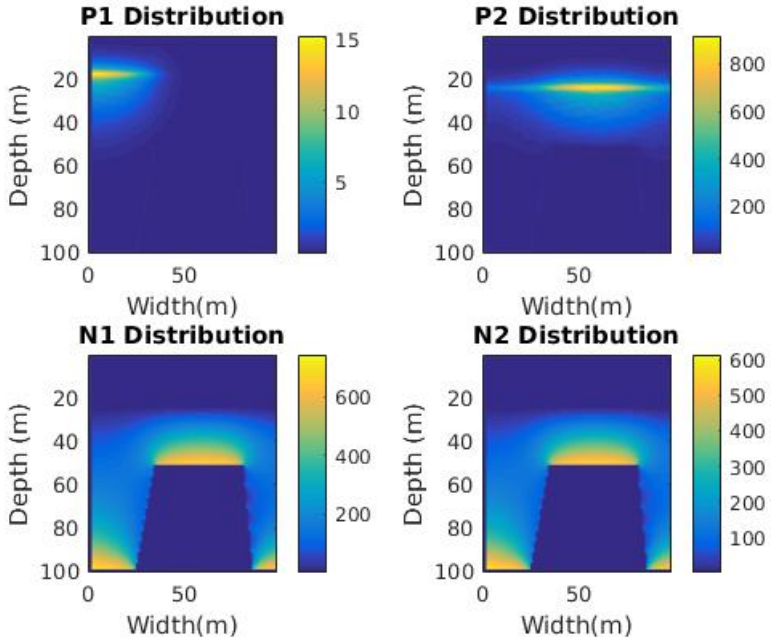

Figure 4.15: 2D population distributions in a slow current with a plateau bound.

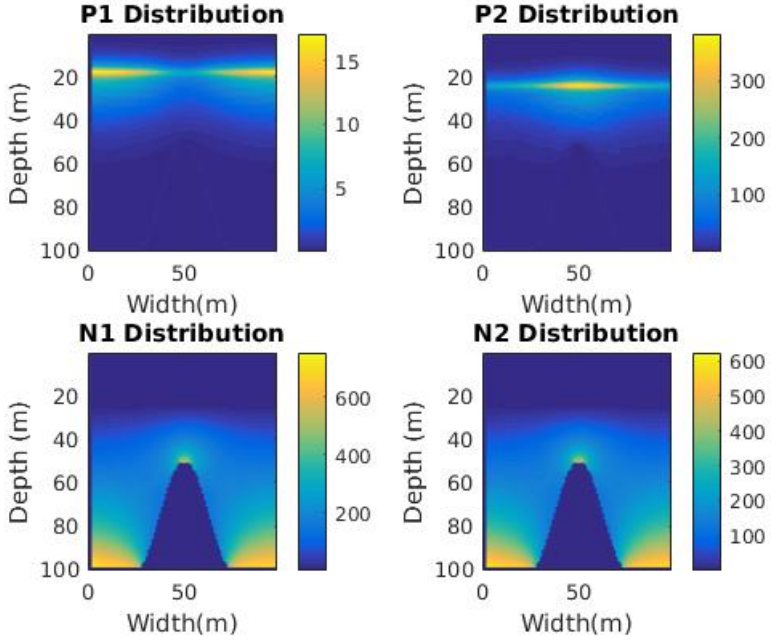

Figure 4.16: 2D population distributions in a slow current with a small hill bound.

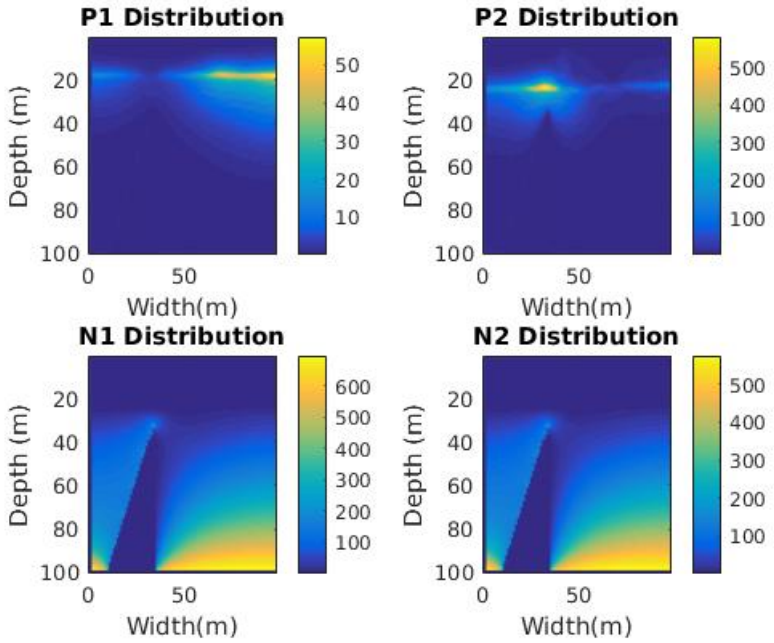

Figure 4.17: 2D population distributions in a slow current with a steep drop-off bound.

could be due to the population of phytoplankton 1 thriving and reaching a level such that it blocked the light from penetrating past its preferred depth. If either phytoplankton population get too large, then the population creates a shade barrier and prevents light from penetrating past its preferred depth.

The plateau, small hill, and drop-off boundaries all appear to have higher concentrations of nutrients along their corresponding hill features when the current has been slowed down. One explanation could be that a faster current pulls the nutrients off of the boundaries and quickly disperses the nutrients into the rest of the system while a slow current does not force the nutrients away from their source, i.e. the sediment and mussels, which allows a build up of nutrients along the hill feature.

Another point of interest is the way the phytoplankton populations are distributed across the width of the area. While the open boundary has a distinctly straight and constant line of phytoplankton concentration across the width of the space, the other boundaries have broken lines of populations. In each bound, one can see that phytoplankton 2 is concentrating towards the middle of the space and directly above the tallest point of the boundary. Recall that phytoplankton 2 requires more nutrients than phytoplankton 1 due

to the assumption that $\kappa_2 > \kappa_1$. The hill feature within the boundary supplies nutrients back into the system and, since phytoplankton 2 needs more nutrients than phytoplankton 1, phytoplankton 2 moves towards the area with the greatest nutrient availability. Phytoplankton 1 does not appear to be able to penetrate the strong concentration of phytoplankton 2 and ends up concentrating to the left and right edges of the hill feature. Phytoplankton 1 still prefers a shallower depth than phytoplankton 1 due to λ_1 being greater than λ_2.

5 Conclusion

The quagga mussel invasion of the Great Lakes is not a problem that will disappear on its own. Quagga mussels have a strong presence in every Great Lake except Lake Superior. The depletion of phytoplankton by the quagga mussels causes waves of disaster throughout the Lake Michigan food web. For example, before the mussel invasion there was about 5,200 Diporeia, a local shrimp-like species, per square meter. After the quagga mussel invasion, Diporeia is down to 82 counts per square meter [24]. The Lake Whitefish, which is a commercial fish species, primarily consumes Diporeia and, due to the loss of population, this commercial fish is no longer abundant enough in Lake Michigan to support a commercial industry.

The quagga mussel is an economic and environmental problem that warrants a great deal of attention. By simulating the biological interactions between phytoplankton, nutrients, and mussels through implementation of the lattice Boltzmann method, this project took a step forward in understanding the relationship between large bathymetric features of the lake, the water current, and the distribution of phytoplankton and nutrients throughout a lake similar to Lake Michigan.

The simulations of this project found that the shape of the bottom boundary impacted the preferred depth of phytoplankton. The addition of a hill-feature to the bottom boundary resulted in phytoplankton preferring a depth shallower than that of an open channel. For

example, the steep drop-off boundary resulted in phytoplankton populations preferring the shallowest depth of 13-20 meters for species 1 and 19-24 meters for species 2 while in the open channel phytoplankton preferred depths of 25 and 33 meters for species 1 and species 2, respectively. The change in preferred depth is most likely associated with the upwelling caused by the change in nutrient conditions above the bathymetric features as well as the changed position of the primary phytoplankton consumer, the quagga mussels. In an open channel, most of the nutrients are concentrated at the lowest depth within the lake sediment. Alternatively, when a hill feature is introduced into the space, the enriched sediment can be found at depths of only 40 meters deep which result in phytoplankton having access to nutrients at a shallower location.

This report also found that the fluid fluxes generated around the boundary greatly influenced the shape of the phytoplankton distribution. Considering first the fluid fluxes generated by the normal current speed, Figures 3.5a - 3.5d, those boundaries with a hill-feature resulted in areas with highly concentrated fluid particle distributions, namely above and to the right the hill, and areas with sparsely distributed fluid particles, namely below and to the right of the hill. The fluid flux pattern was reflected in the shape of the phytoplankton distributions. Figures 4.8, 4.10, and 4.12 have phytoplankton populations that are both curved up towards the surface and have a small proportion of the population dispersing away from the main concentration in the area to the right of the hill. Both the curved feature and the dispersion of particles can be attributed to the hill feature generating curved fluxes as the water current moves up and over the boundary. These effects appear to be enhanced by the chosen speed of the current. Comparing the dispersion of particles and the curved distribution in the previously referenced figures to those in Section 4.4 with a slow current, one can see that the dispersion of the phytoplankton population is greatly diminished and take the shape of a straight line across the area. Thus, it appears that the stronger the current, the greater the phytoplankton population moves with the fluid fluxes generated over the bathymetric feature.

An additional effect of the slow current was a change in the distribution of the phy-

toplankton population throughout the width of the space. When the current is slow, nutrients have a higher concentration along the edges of the hill which resulted in phytoplankton species 2 preferring the space located directly above the tallest point of the hill. This preference from phytoplankton 2 resulted in phytoplankton 1 preferring the areas to the left and right of the hill in order to have direct access to the nutrients below. On the other hand, with a normal current speed, both phytoplankton populations preferred locations above and to the right of the tallest point of the hill. This result could be attributed to the fast current speed causing a greater diffusion of nutrients throughout the space such that the phytoplankton species could inhabit the same location and still have access to the adequate amount of nutrients it needs to thrive.

One limitation of this model are the assumptions made for the biological parameters in Table 1. While all values that were used in this project are found in literature, many parameters have wide ranges of values which can significantly change the results. A future project would entail detailed research into biological parameters for each species. Specifically, the nutrient recycling performed by the mussels, the recycling of deceased biomass in the open water, and the amount of nutrients found in the sediment of the lake could be further analyzed to improve the accuracy of this model.

Improving the thoroughness of this simulation could be accomplished by expanding the model into three dimensions or enlarging the biological model through inclusion of another phytoplankton species, another nutrient, or the next highest species in the food chain like zooplankton or Diporeia. Due to the ease of implementation of suspended particles within the lattice Boltzmann model, additional biological interactions would be straightforward to accomplish. The new biological consumption and growth rates would be implemented into the collision step of this model and the added populations would go through the same streaming step. More detailed biological interactions and the expansion into three dimensions would provide further insight into the relationship of quagga mussels and the aquatic food system of Lake Michigan.

The lattice Boltzmann method proved to be a viable and flexible computational tool for

quantitatively evaluating the impacts bathymetry and currents have on the interactions of two phytoplankton species, two nutrients, and a mussel population of benthic grazers. This simulation and future work towards improving the accuracy of this lattice Boltzmann biological model will contribute to the difficult task of describing the economic and environmental impacts the invasive quagga mussel species has on the aquatic community of Lake Michigan.

6 References

1. Dellacherie, S. (2014). *Construction and Analysis of Lattice Boltzmann Methods Applied to a 1D Convection-Diffusion Equation*, Acta Applicandae Mathematicae, 131,1, pp. 69-140.

2. Eppley, R., Rogers, J., and McCarthy, J. (1969). *Half Saturation Constants for Uptake of Nitrate and Ammonium by Marine Phytoplankton.* Limnology and Oceanography, 14, 6, pp. 912-920.

3. Fahnenstiel, G., Pothoven, S., Vanderploeg, H., Klarer, D., Nalepa, T., and Scavia, D. (2010). *Recent changes in primary production and phytoplankton in the offshore region of southeastern Lake Michigan.* Journal of Great Lakes Research, 36, pp. 20-29.

4. Fillingham, J. H. *Modeling Lake Michigan Nearshore Carbon and Phosphorus Dynamics.* PhD Thesis, University of Wisconsin, Milwaukee, Wisconsin, 2015.

5. Gallivan, M. A., Noble, D. R., Georgiadis, J.G., and Buckius, R. O., (1997). *An evaluation of the bounce-back boundary condition for lattice boltzmann simulations*, International Journal for Numerical Methods in Fluids, 25, 3, pp. 249-263.

6. Greb, S., Garrison, P, and Pfeiffer, S. (2004). *Cladophora and Water Quality of Lake Michigan: A Systematic Survey of Wisconsin Nearshore Areas*, DNR Integrated Science Services and DNR Office of the Great Lakes, Wisconsin.

7. Guo, Z., Shu, C., and Ebrary, Inc. *Lattice Boltzmann Method and Its Application in Engineering.* World Scientific, Singapore, 2013.

8. Haney, J.D., and Jackson, G.A. (1996). *Modeling Phytoplankton Growth Rates.* Journal of Plankton Research, 18, 1, pp. 63-85.

9. Haslam, I. *Lattice Boltzmann Matlab Scripts.* April 9 2016. Web: exolete.com/lbm/.

10. He, X. and Luo, L. (1997). *Theory of the lattice Boltzmann method: From the Boltzmann equation to the lattice Boltzmann equation.* Physical Review, 56, 6, pp. 6811 - 6817.

11. Kerfoot, W. Charles, Yousef, Foad, Green, Sarah A., Budd, Judith W., Schwab, David J., and Vanderploeg, Henry A. (2010). *Approaching storm: Disappearing winter bloom in Lake Michigan.* Journal of Great Lakes Research, 36, pp. 30-41.

12. Klausmeier, C., and Litchman, E. (2001). *Algal games: The vertical distribution of phytoplankton in poorly mixed water columns.* Limnology and Oceanography, 46,8,pp. 1998-2007.

13. Ladd, A. (1994). *Numerical Simulations of Particulate Suspensions via a Discretized Boltzmann Equation Part I Theoretical Foundation.* Journal of Fluid Mechanics, 271, pp. 285-309.

14. Lake Access. *Understanding Lakes:Light.* An EMPACT Metro Project, http://www.lakeaccess.org/ecology/lakeecologyprim3.html, (April 10 2016)

15. Lake Michigan Studies: Biological Investigations. Great Lakes IL River Basins Project. US Department of Health Education and Welfare, Public Health Service, Division of Water Supply and Pollution Control. Special Report Number IM 4.

16. Lessin, G.,Lips, I., and Raudsepp, U. (2007). *Modelling nitrogen and phosphorus limitation on phytoplankton growth in Narva Bay South Eastern Gulf of Finland.* Oceanologia, 49,2, pp. 259-276.

17. Link, C., (2010). *Filtration and Growth Rate of Lake Mead Quagga Mussels (Dreissena Bugensis) in Laboratory Studies and Analyses of Bioaccumulation*, Masters Thesis, University of Nevada, Las Vegas, Nevada.

18. Makarewicz, J., Lewis, T., and Betram, P.E. (1989). *Phytoplankton and zooplankton composition, abundance and distribution and trophic interactions : Offshore region of Lakes Erie, Lake Huron and Lake Michigan* USEPA: Great Lakes Na-

tional Program Office, Report No. 01-91, Chicago, Illinois.

19. Makarewicz, J.C., Bertram, P., and Lewis, T. W. (1998). *Changes in Phytoplankton Size Class Abundance and Species Composition Coinciding with Changes in Water Chemistry and Zooplankton Community Structure of Lake Michigan 1983 to 1992.* J. Great Lakes Res, 24, 3, pp. 637-657.

20. Mei, R., Shyy, W., Yu, D., and Institute for Computer Applications In Science Engineering Hampton VA. (2002). *Lattice Boltzmann Method for 3-D Flows with Curved Boundary.*

21. Mele, I. (2013). *Lattice Boltzmann method.* Seminar, Univerza v Ljublijani.

22. Mellard, J.P., Yoshiyama, K., Litchman, E., and Klausmeier, C.A. (2011). *The vertical distribution of phytoplankton in stratified water columns.* Journal of Theoretical Biology, 269, 1, pp. 16-30.

23. NOAA. *Great Lakes Data Rescue Project: Lake Michigan Bathymetry*, https:// www .ngdc .noaa .gov /mgg /greatlakes /lakemich _ cdrom /html /geomorph (April 11 2016).

24. Nalepa, T.F., Fanslow, D. L., Lang,G.A., Lamarand, D.B., Cummins,L.G. , and Carter,G.S. (2008). *Abundance of the amphipod Diporeia and the mussels Dreissena polymorpha and Dreissena rostriformis bugensis in Lake Michigan in 1994, 2000, and 2005.* NOAA Technical Memorandum GLERL-144. Ann Arbor, Michigan.

25. Nalepa, T.F., Fanslow, D.L., and Pothoven, S.A. (2010). *Recent changes in density, biomass, recruitment, size structure, and nutritional state of Dreissena populations in southern Lake Michigan.* Journal of Great Lakes Research, 36, pp. 5-19.

26. Prins, T.C., Smaal, A.C., Dame, R.F., and Centre for Estuarine and Marine Ecology. (1998). *A review of the feedbacks between bivalve grazing and ecosystem processes.* Aquatic Ecology, 31, pp. 349-359.

27. Qi, D., and Luo, L. (2003). *Rotational and orientational behaviour of three-dimensional spheroidal particles in Couette flows.* Journal of Fluid Mechanics, 477, pp. 201-213.

28. Qian Y.H., DHumieres, D., and Lallemand, P. (1992).*Lattice BGK Models for Navier Stokes Equation.* Europhysics Letters, 17, 6, pp. 479.

29. Rowe, M., Obenour, D., Nalepa, T., Vanderploeg, H., Yousef, F., and Kerfoot, W. (2015). *Mapping the spatial distribution of the biomass and filter feeding effect of invasive dreissenid mussels on the winter-spring phytoplankton bloom in Lake Michigan.* Freshwater Biology, 60, 11, pp. 2270-2285.

30. Smith, A., Nikora, V., Ross, A., and Wake, G. (2006). *A lattice Boltzmann-based model of plankton–flow interaction around a mussel cluster*, Ecological Modeling, 192,3, pp. 645-657.

31. Stoeckmann, A. (2003). *Physiological energetics of Lake Erie dreissenid mussels: A basis for the displacement of Dreissena polymorpha by Dreissena bugensis.* Canadian Journal of Fisheries and Aquatic Sciences, 60,2, pp. 126-134.

32. Stojsavljevic, T. (2014). *Mathematical Modeling of Competition for Light and Nutrients Between Phytoplankton Species in a Poorly Mixed Water Column.* Masters Thesis, University of Wisconsin, Milwaukee, WI.

33. Strayer, D., Caraco, N., Cole, J., Findlay, S., and Pace, M. (1999). *Transformation of Freshwater Ecosystems by Bivalves. A case study of zebra mussels in the Hudson River.* BioScience, 49, 1,pp. 19-27.

34. Sucsy, P., Hendrickson, J. (2003). *Calculation of Nutrient Reduction Goals for the Lower St. Johns River by Application of CE-QUAL-ICM, a Mechanistic Water Quality Model.* Department of Water Resources, Florida.

35. Tang, H., Vanderploeg, H. A., Johengen, T. H., and Liebig, J.R. (2014). *Quagga mussel, Dreissena rostriformis bugensis, selective feeding of phytoplankton in Saginaw Bay.* Journal of Great Lakes Research, Supplement 40, pp. 83-94.

36. Tyner, E. H., Bootsma, H.A., and Lafrancois, B.M.(2014). Dreissenid metabolism and ecosystem-scale effects as revealed by oxygen consumption. Journal of Great Lakes Research,41 Supplement 3, pp. 27–37

37. Vaughn, C., Nichols, S., and Spooner, D. (2008). *Community and foodweb ecology of freshwater mussels.* Journal of the North American Benthological Society, 27, 2,pp. 409-423.

38. Wetstein, T. (2014). *Implementing the lattice Boltmann Method: A Research on Implementation Techniques.* Bachelors Thesis, Delft University of Technology, South Hollands.

39. Yu, D., Mei, R., Lio, L., and Shyy, W. (2003). *Viscous flow computations with the method of lattice Boltzmann equation*,Progress in Aerospace Sciences,39, pp. 329-367.

40. Zhai, L., Platt, T., Tang, C., Dowd, M., Sathyendranath, S., and Forget, M. (2008). *Estimation of phytoplankton loss rate by remote sensing.* Geophysical Research Letters, 35, 23.